Nanotechnology **21** (2010) 075602 (7pp) doi:10.1088/0957-4484/21/7/075602

In situ monitoring of single-wall carbon nanotube laser assisted growth

Miro Haluška[1,3,4], Yves Bellouard[1,4], Yoeri van de Burgt[1,2] and Andreas Dietzel[1,2]

[1] Micro- and Nano-scale Engineering, Department of Mechanical Engineering, Eindhoven University of Technology, Den Dolech 2, 5600 MB Eindhoven, The Netherlands
[2] Holst Centre/TNO, High Tech Campus 31, PO Box 8550, 5605 KN Eindhoven, The Netherlands

E-mail: haluska@micro.mavt.ethz.ch and y.bellouard@tue.nl

Received 11 November 2009, in final form 21 December 2009
Published 18 January 2010
Online at stacks.iop.org/Nano/21/075602

Abstract
Laser assisted catalytic chemical vapor deposition has recently emerged as an attractive method for locally growing carbon nanotubes (CNTs) in a cold wall reactor. So far, reported laser assisted CNT growth has been carried out without *in situ* process monitoring. This has made it difficult to control the growth process and limits the applicability of the method. Using a set of photodetectors with different spectral responses, we show that one can identify characteristic regimes of laser assisted CNT growth. More specifically, key process steps like catalyst activation, growth of CNTs, and amorphous carbon deposition are identified. Furthermore, the method allows optimization of growth conditions with respect to the quality of the growth products.

(Some figures in this article are in colour only in the electronic version)

1. Introduction

Laser assisted catalytic chemical vapor deposition (LA CCVD) has recently gained attention as a suitable process for growing carbon nanotubes (CNTs) locally on 'cold substrates'. LA CCVD is of particular interest for applications where classical chemical vapor deposition (CVD) processes are not suitable due to temperature sensitive elements present on the substrate. It is also a promising, maskless technology that can replace catalyst patterning. Furthermore, different CNT assemblies requiring different processing parameters can be grown on a single substrate. Successful LA CCVD growth of CNTs has been reported by several authors [1–6]. In [7], we reported the growth of a forest of vertically aligned single-wall carbon nanotubes (SWCNTs) utilizing LA CCVD. So far, these results are laboratory ones. To industrialize the process, a key requirement will be the ability to control the process. In particular, one will have to detect both onset and termination of the CNT growth.

Here we use a set of photodetectors with different spectral responses in the near-infrared and visible ranges to identify characteristic regimes of the LA CCVD growth of CNTs: namely, activation of catalysts, CNT growth and amorphous carbon deposition which terminates the nanotube growth. To identify the growth products obtained for a given set of exposure conditions, we collected *ex situ* Raman spectra and scanning electron microscope (SEM) images of the laser-affected zones. Thanks to these observations, we identified photodetector signal patterns that we can correlate with the onset of nanotube growth and the occurrence of amorphous carbon deposits. This is a very important step towards the efficient monitoring and *in situ* control of the LA CCVD process. We expect this result to have significant implications for instance for CNT-based flexible electronics (see [8]). Furthermore, the process *in situ* diagnosis allows us to optimize the experimental conditions with respect to the quality of the growth products.

2. Experimental details

Our LA CCVD process takes place in a small stainless steel reactor with a volume of 3.4 l (figure 1). The reactor contains

[3] Present address: Micro and Nanosystems, Department of Mechanical and Process Engineering, ETH Zürich, CLA H1, Tannenstrasse 3, 8092 Zurich, Switzerland.
[4] Authors to whom any correspondence should be addressed.

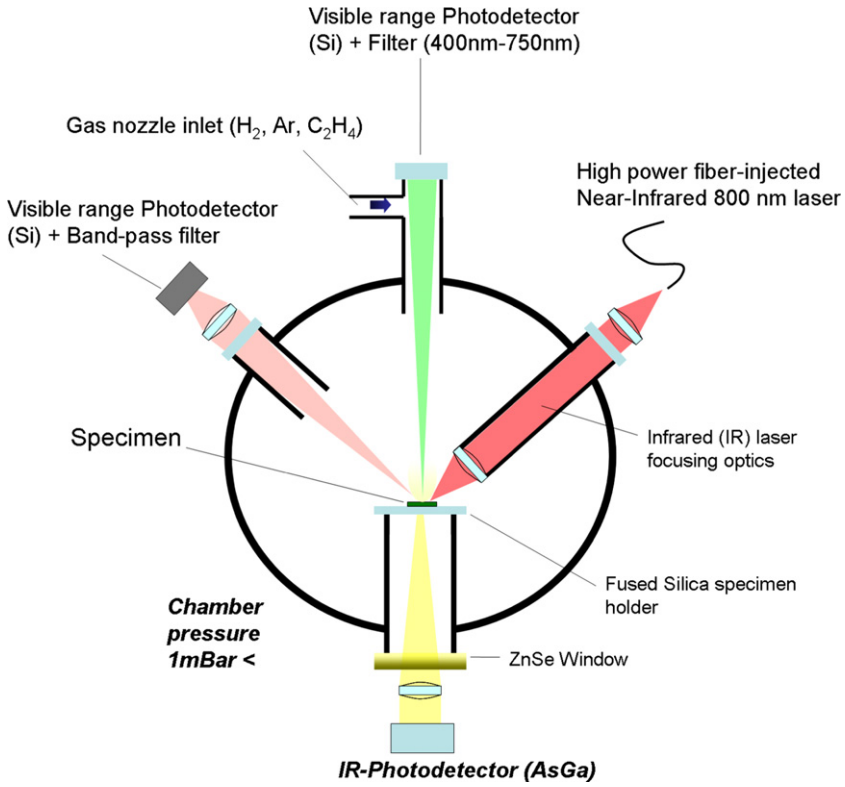

Figure 1. Schematic of the LA CCVD reactor equipped with detectors for *in situ* measurements of the substrate temperature as well as the intensities of reflected and emitted light.

a gas inlet and outlet, temperature and pressure sensors, three windows for *in situ* optical observation, a horizontal substrate holder and an optical assembly that focuses the laser beam on the substrate at a 35° incidence angle. We use a laser diode (from Unique-mode AG) continuously emitting at 800 nm, with a maximal optical power of 35 W. The laser beam intensity and the spot size can be tuned independently, offering the possibility of growing CNT assemblies of different sizes and types (MWCNTs or SWCNTs). Three photodetectors are used to detect visible light emitted from the CNTs, reflected laser beam light from the substrate and infrared emission (i.e. thermal radiation) from the back of the substrate (figure 1).

The first photodetector (a Si fast photodiode, DET210 from Thorlabs Inc., USA), combined with a laser line band-pass filter centered at 800 nm with a spectral width of about 10 nm is used to measure the reflected laser light from the substrate. The objective is to dynamically measure the changes of reflectivity, which indicate surface topography changes or increased absorption on the surface.

The second photodetector, a GaAs photodiode (from Thorlabs Inc., USA, DET410), with a spectral response spread from 700 to 1800 nm, is used to analyze the signal in the near-infrared range from the back of the substrate. The origin of this infrared radiation is essentially thermal (the Si substrate is not transparent for wavelengths below 1 μm) and provides an indication of local temperature changes. We later refer to this photodetector by as the 'IR signal detector'.

The third photodetector is another Si photodiode combined with a low-pass filter that cuts wavelengths above 750 nm. This third sensor, located ∼20 cm above the substrate, is used to analyze emitted visible light from the irradiated spot (CNTs) in a direction perpendicular to the substrate.

In addition to these optical sensors, a thermocouple is placed 0.8 mm from the laser spot in contact with the periphery of the substrate. This thermocouple is later used for calibrating our thermal model that is used to estimate the temperature at the laser spot. Furthermore, the thermocouple measurement allows us to cross-check the information collected using the IR signal photodetector.

The specimens used were silicon substrates (0.7 mm thick) covered with a 20 nm thick layer of Al_2O_3. Either 1.5 or 1.8 nm thick Fe layers were sputtered on top. The specimens were mounted horizontally on a fused silica holder. The chamber was pumped down to approximately 10^{-3} mbar and subsequently filled with a mixture of argon, hydrogen, and ethylene (in a ratio of 8:2:5) until the chamber reaches ambient pressure. The laser spot was an ellipsoid with dimensions of 118 μm × 96 μm.

Raman spectroscopy and scanning electron microscopy (SEM) were used to characterize the as-grown products. Raman spectra were measured using a Jobin-Yvon LabRam spectrometer equipped with a 633 nm excitation wavelength. SEM images were obtained with a field emission gun Environmental XL 30 ESEM-FEG Philips scanning electron microscope.

To interpret the photodetector signals and identify characteristic regimes, we compared *in situ* and *ex situ* obtained data for each specimen. For a given set of the

specimens, a series of repetitive experiments were carried out with the same process parameters but with different laser exposure times.

3. Results and discussion

3.1. Detection of the onset of CNT growth

Figures 2(a) and (b) show both the temperature and the intensity of reflected light as a function of laser irradiance. Blue stars and red bullets are data points obtained in an Ar/H_2 atmosphere, without and with a carbon containing gas (here ethylene, C_2H_4), respectively. The experiments were done on Si/Al_2O_3 substrates coated with a 1.5 nm Fe film. The black crosses represent signals measured on a pre-existing CNT forest when ethylene was absent (in an Ar/H_2 atmosphere). For the data shown in figure 2, the laser irradiance (optical power density) was increased stepwise at an average rate of 0.19 W min^{-1}. Without ethylene in the reactor, the reflected light intensity increased nearly linearly until the substrate surface became damaged. When ethylene (together with Ar and H_2) is present in the reactor, abrupt changes of temperature and reflected light intensity are observed at about 6.2×10^4 W cm^{-2}. Immediately after observing these sharp changes, the laser irradiance was manually decreased. As can be seen in figure 2, the temperature and intensity of the reflected light then mimic the behavior of a substrate with an already present vertically aligned forest of CNTs and exposed to the same laser irradiation. SEM observations of the as-grown product show a dome structure made of nanotubes covered with amorphous carbon. From these observations, we concluded that the significant changes in the substrate temperature and the intensity of reflected light are characteristics for the onset of the CNT growth.

This important observation opens new opportunities for a feedback controlled process in which laser light is not only used as a heating tool but also for *in situ* detection of the CNT growth onset.

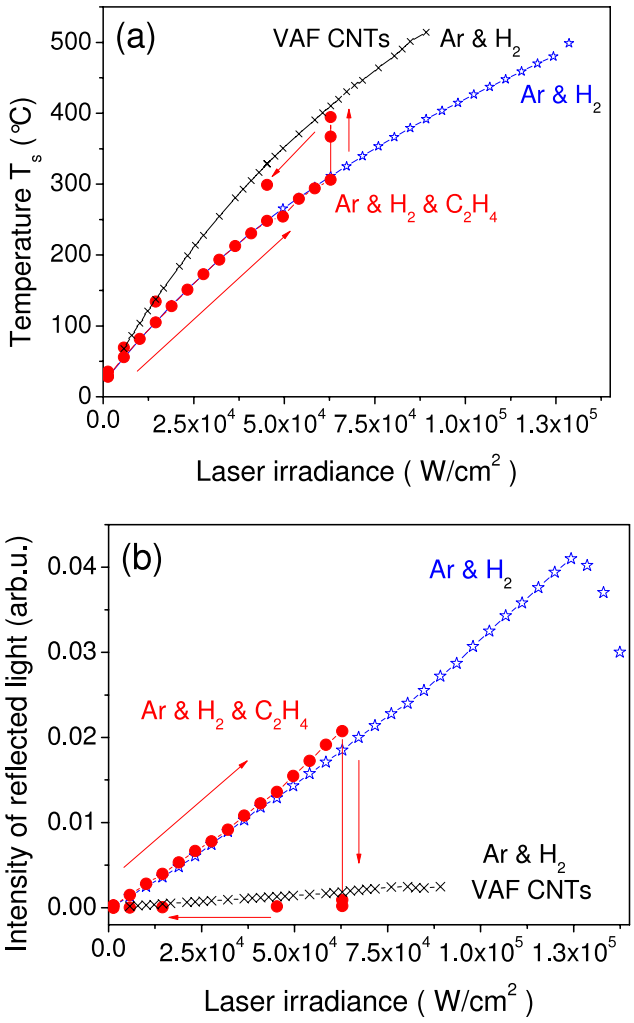

Figure 2. (a) Temperature of three substrates measured *in situ* by a thermocouple and (b) the corresponding intensities of the reflected light. Blue stars and red bullets represent the experiments done in $Ar + H_2$ and $Ar + H_2 + C_2H_4$ atmospheres, respectively. Black crosses represent the measurements in $Ar + H_2$ for a reference sample of pre-grown VAF CNTs.

3.2. Optimal irradiance level

Si/Al_2O_3/Fe substrates reflect more than 20% of incoming light as concluded from the measurement of the optical power. A vertically aligned forest of CNTs has very low reflectance as shown in [9]. The decrease of the reflected light intensity caused by the growth of VAF CNTs was also shown by Puretzky *et al* [10]. An increase of absorbed laser radiation in the CNTs raises the sample temperature and simultaneously increases the non-catalytically activated rate of thermal decomposition of ethylene. Consequently, amorphous carbon is deposited on the CNTs and catalyst particles preventing the growth of CNTs.

The LA CCVD process is characterized by a very fast temperature elevation at the laser spot, which helps to transform the metal film into small catalyst particles required for the SWCNT nucleation and growth. These densely packed clusters form the seed structure for vertically oriented SWCNTs.

Rather than slowly increasing the temperature as described in the previous paragraph (and shown in figure 2), here we steeply increased the laser irradiance of the substrate in a single step. This allows us to recreate the conditions for 'flash' heating necessary for the formation of small clusters on which SWCNTs can grow.

To find the optimal irradiance level for SWCNT growth, we performed several experiments at different irradiance levels. Figure 3(a) shows the Raman spectra of CNTs grown on Si/Al_2O_3/1.8 nm Fe substrates for different laser irradiances. The exposure time was 10 s for all the experiments except for the one performed at the lowest irradiance, where the exposure time was 15 s. In figure 3(a), Si labels indicate silicon substrate Raman modes, G and D^* are modes corresponding to sp^2 hybridized carbon and D is the mode allowed in sp^2 hybridized carbon only if defects are present [11, 12]. It is well known that the level of graphitization is proportional to the growth temperature [13]. Further, the radial breathing mode (RBM)

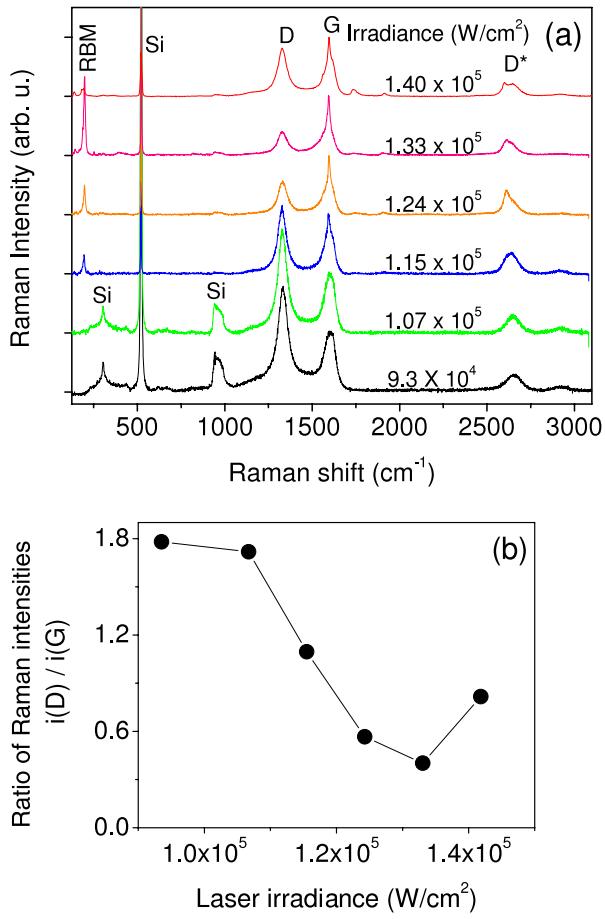

Figure 3. (a) Raman spectra of CNTs prepared at different laser irradiances on substrates with a 1.8 nm Fe film. The curves are shifted in the vertical direction for clarity. The level of irradiance is indicated next to each spectrum. (b) Ratio of Raman intensities of the D and the G modes from (a).

together with the position and shape of the G mode indicate the presence of SWCNTs.

Figure 3(b) shows the ratio of the D mode and the G mode intensities of the Raman spectra. The ratio is, in a first approximation, a measure of the graphitization level of nanotubes or, in other words, a sign of the CNT wall quality (i.e. the lower the ratio the higher the quality of the CNT walls). Both figures 3(a) and (b) indicate that for low laser irradiance more defects in the CNT wall are formed. Above $\sim 1.2 \times 10^5$ W cm^{-2}, SWCNTs are found. The dominant RBM mode at ~ 198 cm^{-1} represents SWCNTs with diameter ~ 1.2 nm. Above 1.33×10^5 W cm^{-2}, the ratio $i(\mathrm{D})/i(\mathrm{G})$ increases, indicating that this irradiance level induces the formation of defects in the nanotubes. Another possible explanation for the increase of the $i(\mathrm{D})/i(\mathrm{G})$ ratio is that at the high irradiance level the temperature at the center of the laser spot increases above the threshold limit for thermal non-catalytic dissociation of ethylene and amorphous carbon formation.

3.3. Identification of the growth regimes during laser exposure

Figures 4(a)–(c) show SEM images of three samples irradiated with the power density of 1.07×10^5 W cm^{-2} for three different exposure times of 8, 10.5 and 16 s, respectively. From these observations, various growth regimes could be identified. Figures 4(a) and (b) display the clusters formed from a Fe film after 8 s and CNTs obtained after 10.5 s of laser exposure, respectively. For the latter, the nanotubes grew probably partly also in a short time period after the laser was turned off while the substrate was cooling down. Lower temperature may have caused the growth of lower quality nanotubes. This is clearly visible in the Raman spectrum with a high D–G intensity ratio shown with the black line (lower curve) in figure 4(f). Figure 4(c) shows VAF SWCNTs found after 16 s laser irradiation time. Here, the presence of SWCNTs is confirmed with a red line (upper curve) Raman spectrum in figure 4(f). Figures 4(d) and (e) show the temperature and its time derivative for the three samples, respectively. Temperature starts to decrease after switching off the laser. The evolutions of the temperature are very similar and reproducible for the experiments.

Next, to further improve our LA CCVD process and to better interpret the *in situ* data collected with various optical sensors, we performed a set of experiments to correlate *in situ* measurements with *ex situ* observations.

Figure 5 shows normalized signals of the reflected light intensity, the substrate temperature, the time derivative of the temperature as well as the IR and visible emitted light signals, obtained during a constant laser irradiance of the substrate. We note three different regimes.

3.3.1. Regime I: Fe restructuring. During this time period, the Fe film melts locally and forms clusters of catalyst nanoparticles (an example is shown in figure 4(a)). Fluctuations in the photodetector signals are observed but remain difficult to interpret. This stage is attributed to the catalyst activation and may have variable duration depending on the laser irradiation power density (that controls the temperature of the laser-affected area) as well as on the metal film thickness. Rather than measuring the temperature of the irradiated area which is technically challenging, we use the local minima of the time derivative of the temperature measured using the thermocouple to identify the onset time for the CNT growth.

Figure 6(a) shows the log–log dependence of the onset time for CNT growth as a function of the heating rate as measured using the thermocouple. Slow heating rates (slower than 22 °C s^{-1}) were obtained by gradually increasing the laser power whereas the higher heating rates were achieved by applying a step-like power increase as mentioned above. The figure shows that the catalyst activation needs a longer time for slower heating rates. Using an Arrhenius equation, the energy for the catalyst activation can be estimated. For this, we calculated the rate constants as an inverse of the onset times. The temperature at the center of the laser spot was calculated from a heat transfer model (using finite element modeling). The activation energy is estimated to be ~ 0.35 eV for onset times of 16 s and shorter.

Figure 6(b) shows various Raman spectra for specimens prepared at high (upper curve), intermediate (middle curve) and slow (lower curve) heating rates. Fast heating rates cause

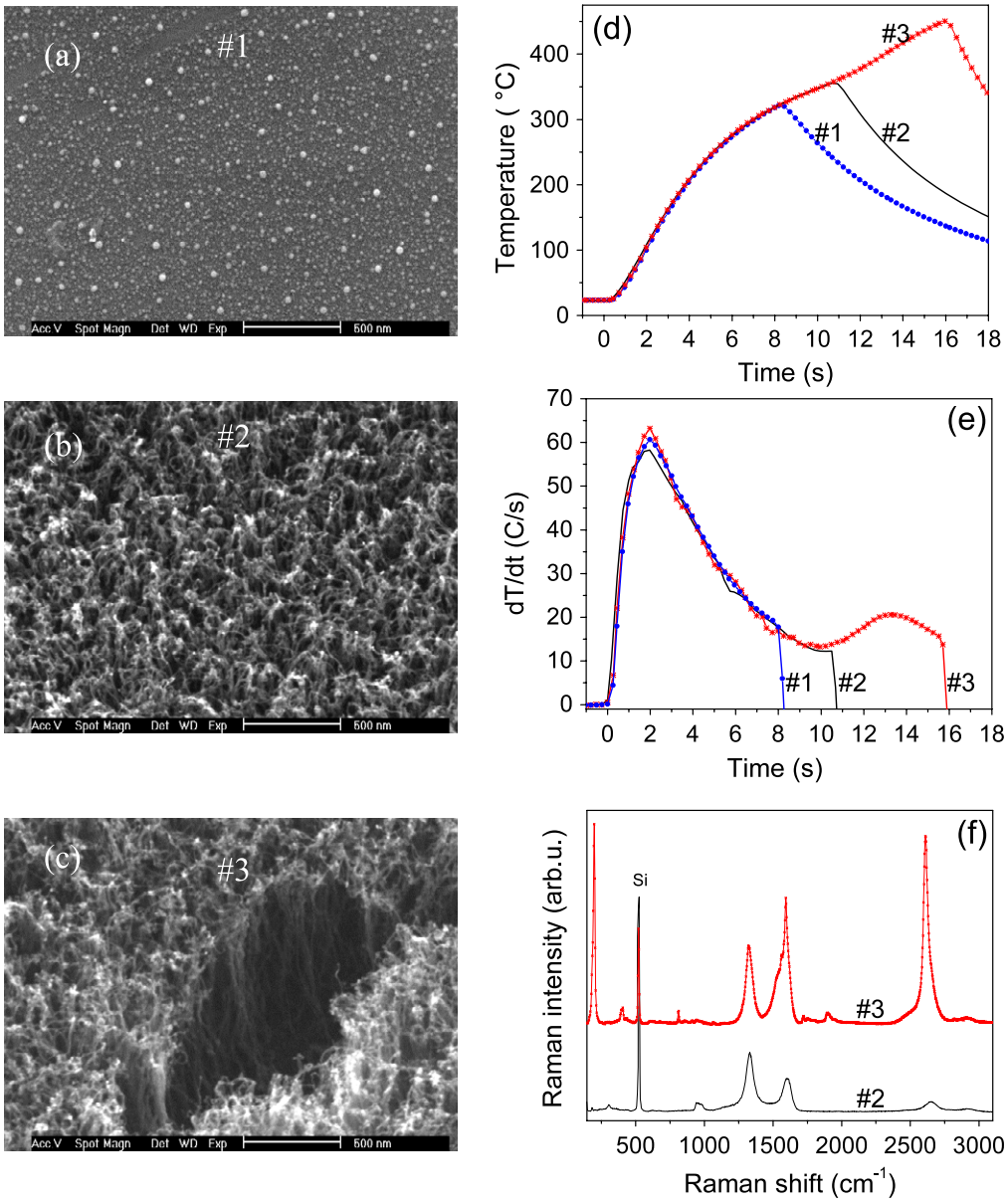

Figure 4. Effect of irradiation time on CNT growth. Three irradiation times are considered: 8, 10.5 and 16 s, labeled (#1), (#2) and (#3), respectively. ((a)–(c)) SEM images, (d) temperature, (e) time derivative of the temperature, and (f) Raman spectra (shifted in the vertical direction for clarity). Note that the Raman spectrum for sample #1 is not plotted because it does not show presence of carbon mods.

the formation and growth of SWCNTs while slow heating rates yield low quality MWCNTs. The Raman spectra for specimens prepared at the intermediate heating rate indicates the presence of both SWCNTs and MWCNTs.

3.3.2. Regime II: CNT growth. We identify a second regime triggered by a steep drop in reflected light intensity (blue crosses in figure 5). The temperature measured using the thermocouple (red bullets) goes through an inflexion point after which the heating rate increases again. This temperature change is also observed with the IR photodetector (orange triangles). We attribute this second regime to the growth of a CNT forest (figure 4(c)).

3.3.3. Regime III: amorphous carbon deposition. The onset of the final regime is defined by an increase of emitted light followed by a slight increase of the reflected light intensity. This regime seems to be directly correlated with the formation of an amorphous layer that covers the CNT forest. This amorphous deposit is shown in figure 7. It terminates the growth of nanotubes and has a very interesting morphology that resembles frozen liquid droplets. We note that similar carbon spherical objects were reported for thermal non-catalyst activated dissociation of acetylene during chemical vapor deposition [14]. For this stage, we also notice an increase of the visible light intensity emitted from the specimen (green squares in figure 5).

3.4. Correlation between photodetector signals

A set of experiments with (1) Si/Al_2O_3 in $Ar/H_2/C_2H_4$, (2) Si/Al_2O_3/1.5 nm Fe in air, (3) Si/Al_2O_3/1.5 nm Fe in an $Ar/H_2/C_2H_4$ atmosphere, and (4) pre-prepared VAF CNTs in

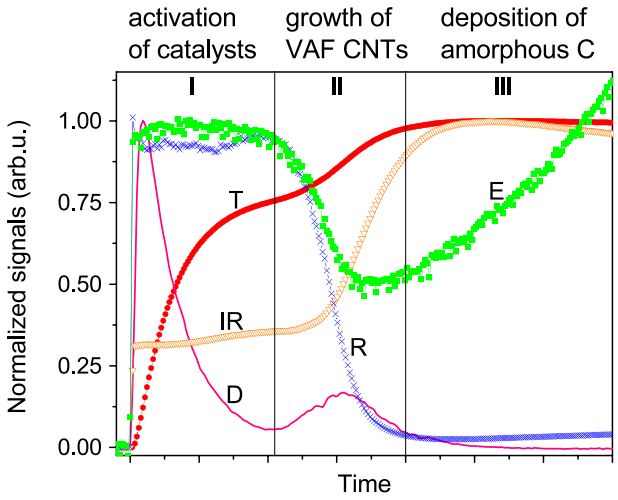

Figure 5. Normalized *in situ* signals that characterize the growth process. The red bullets, the blue crosses, the orange triangles and the green squares represent the temperature (T), the intensity of reflected light (R), the IR detector signal (IR), and the visible light detector signal (E), respectively. The pink curve displays the time derivative of the temperature signal (D). The Roman numbers represent the process regimes.

an Ar/H_2 atmosphere were performed. The growth of CNTs is expected only on the substrate (3). Figures 8(a) and (b) show the time evolution of signals detected by the detector operating in the visible range and the detector of reflected light, respectively. We note a simultaneous drop of the signals and the onset of CNT growth for the sample (3). For reflected light, the intensity drop depends on the height and the density of VAF CNTs and was explained in [9, 10]. The lowest measured intensity is comparable to that for the reference sample of pre-grown VAF CNTs (sample (4)). For the signal detected by the visible range photodetector (sample (3) in figure 8(a)) the intensity decrease is likely due to the filter that does not completely cut off the wavelength of the laser line and still allows the scattered light to enter the photodetector. We assume that the growing CNTs limit the light scattering as compared to the pristine substrate surface prior to the nanotube growth.

As the total energy absorbed by the sample during the regime II increases (as indicated by the decrease of reflected light) the temperature in the laser spot increases and, consequently, CNTs thermally emit more light in the visible spectrum. This increase is clearly evident for the last stage of regime II and in regime III in figures 5 (green squares, curve E). At this stage, to keep the amorphous carbon impurity at a low level, it is necessary to decrease (or switch off) the laser intensity to maintain the nanotubes at a temperature below the threshold for thermal dissociation of ethylene.

4. Conclusion

Laser assisted catalytic chemical vapor deposition (LA CCVD) is an attractive process for growing carbon nanotubes locally. In this paper, we have demonstrated the use of photodetectors to monitor and detect the onset and termination of vertically aligned single-wall carbon nanotube forest growth. Three signals are monitored: the intensity of the laser reflected light, the infrared light emitted from the back of the substrate and

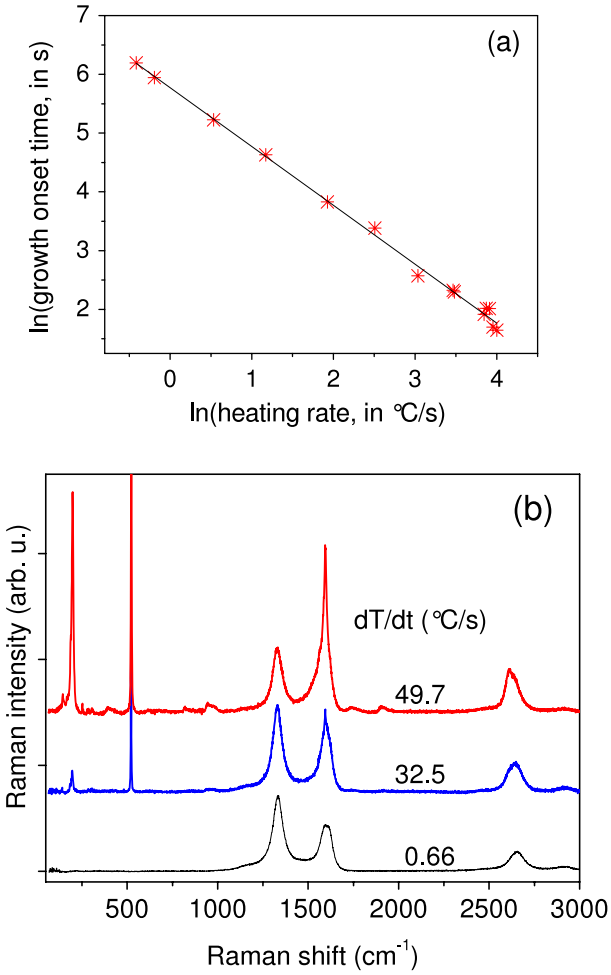

Figure 6. (a) The dependence of the onset for the CNT growth on the heating rate. The symbols correspond to the inflexion points for the temperature versus time curves for different heating rates. (b) Raman spectra obtained for the samples produced at different heating rates. The heating rates are indicated.

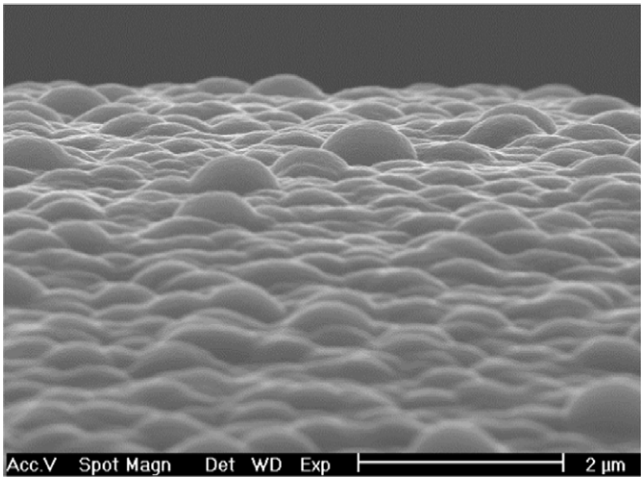

Figure 7. SEM image of a top layer covering the center of a vertically aligned forest of CNTs.

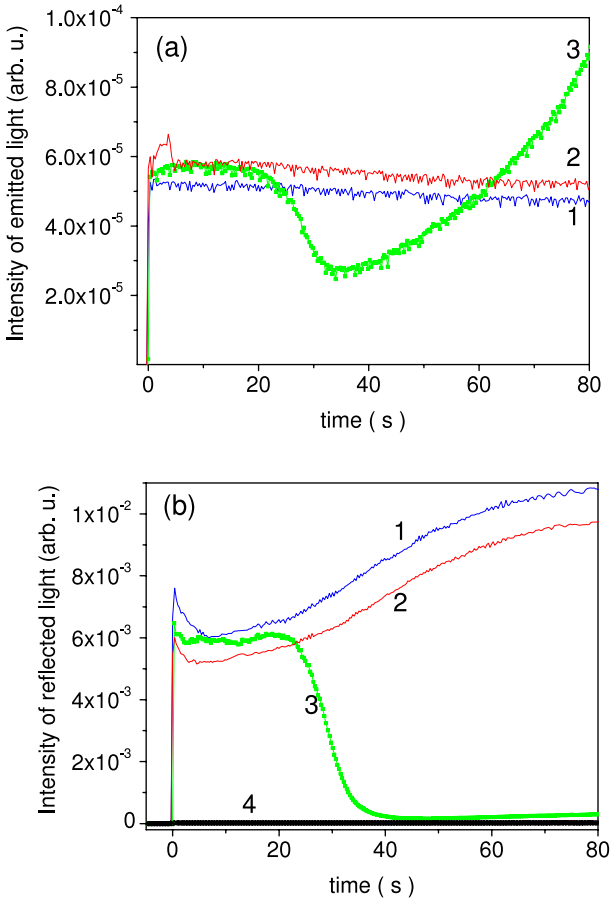

Figure 8. Intensities of (a) emitted and (b) reflected light obtained for (1) Si/Al_2O_3 and (3) Si/Al_2O_3/1.5 nm Fe both in an $Ar/H_2/C_2H_4$ atmosphere, (2) Si/Al_2O_3/1.5 nm Fe in air, and (4) the reference sample of pre-grown VAF CNTs in an Ar/H_2 atmosphere.

the visible light emitted from the surface in a direction normal to the substrate plane. We identify three different regimes during laser exposures: (I) structuring/activation of catalysts, (II) growth of CNTs and (III) deposition of amorphous carbon. Further, we identify an irradiance level for achieving a higher quality of the vertically aligned forest of SWCNTs.

The detected optical signals can be efficiently used for controlling the process of CNT growth. Furthermore, one can use these process monitoring signals to reduce the CNT contamination by amorphous carbon.

Acknowledgments

The authors are grateful to the J Hart University of Michigan and the S Roth group from FKF-MPI Stuttgart for providing some of the Si substrates, to A Schulz from FKF-MPI and to J Laven from STO TU/e for helping out with the Raman experiments, to P Moodley from STO TU/e for providing reference specimens of VAF CNTs, to M Hulman for valuable discussions and, finally, to Willy ter Elst for his help in setting up the LA CCVD chamber and the laboratory.

References

[1] Alexandrescu R, Crunteanu A, Morjan R-E, Morjan I, Rohmund F, Falk L K L, Ledoux G and Huisken F 2003 *Infrared Phys. Technol.* **44** 43
[2] Bondi S N, Lackey W J, Johnson R W, Wang X and Wang Z L 2006 *Carbon* **44** 1393
[3] Chen Z, Wie Y, Luo C, Jiang K, Zhang L, Li Q and Fan S 2007 *Appl. Phys. Lett.* **90** 133108
[4] Fujiwara Y, Maehashi K, Ohno Y, Inoue K and Matsumoto K 2005 *Japan. J. Appl. Phys.* **44** 1581
[5] Shi J, Lu Y F, Yi K J, Lin Y S, Liou S H, Hou J B and Wang X W 2006 *Appl. Phys. Lett.* **89** 083105
[6] Kasuya K, Nagato K, Jin Y, Morii H, Oor T and Nakao M 2007 *Japan. J. Appl. Phys.* **46** L333
[7] Haluska M, Bellouard Y and Dietzel A 2008 *Phys. Status Solidi* a **10** 1927
[8] Tsai T Y, Lee C Y, Tai N H and Tuan W H 2009 *Appl. Phys. Lett.* **95** 013107
[9] Yang Z-P, Ci L, Bur J A, Lin S-Y and Ajayan P M 2008 *Nano Lett.* **8** 446
[10] Puretzky A A, Geohegan D B, Jesse S, Ivanov I N and Eres G 2005 *Appl. Phys.* A **81** 223
[11] Dresselhaus M S and Eklund P C 2000 *Adv. Phys.* **49** 705
[12] Ferrari A C 2007 *Solid State Commun.* **143** 47
[13] Loiseau A, Blase X, Charlier J-Ch, Gadelle P, Journet C, Laurent Ch and Pegney A 2006 *Lect. Notes Phys.* **677** 49
[14] Wu H-C, Hong C-T, Chiu H-T and Li Y-Y 2009 *Diamond Relat. Mater.* **18** 601